View Online / Journal Homepage
Dynamic Article Links

Soft Matter

Cite this: DOI: 10.1039/c2sm06885k

www.rsc.org/softmatter

PAPER

Solid particles in an elastomer matrix: impact of colloid dispersion and polymer mobility modification on the mechanical properties

Aurélie Papon,*[a] Hélène Montes,[a] François Lequeux,[a] Julian Oberdisse,*[b] Kay Saalwächter[c] and Laurent Guy[d]

Received 3rd October 2011, Accepted 3rd February 2012
DOI: 10.1039/c2sm06885k

The reinforcement of elastomers by inorganic fillers, a concept of very high technological importance, is commonly understood to result from the presence of a mechanical network of partially aggregated filler particles. The non-linear mechanical properties, in particular the decrease of the modulus at high strain (Payne effect), are further interpreted to be a consequence of the breakdown of this filler network. There are, however, many open questions concerning the actual nature of the interparticle connections, where a modified polymer layer forming "glassy bridges" constitutes one possibility. In this work, we address this issue with a suitable silica-filled model elastomer, where we characterize the silica dispersion by SANS in combination with reverse Monte-Carlo modeling, and the mobility modification of the polymer by low-field proton NMR spectroscopy. In our samples, we identify a glassy layer as well as a region of intermediate mobility (possibly modified Rouse modes). Based on the structural information from SANS, we are able to quantify the amount of interparticle connections, and correlate it with the magnitude of the Payne effect taken from shear rheology. This works only if we assume that these connections comprise both, the glassy layer as well as the region of intermediate mobility. The amount of glassy immobilized polymer only does not suffice to explain the mechanical properties.

I. Introduction

Dispersing solid fillers into an elastomer matrix is a well-known method to improve the mechanical properties of elastomers for industrial applications such as tyres. In particular, the reinforcement induced by the solid particles increases significantly the abrasion resistance. However, as the amplitude of the reinforcement depends on the temperature, it is clear that this is not a simple hydrodynamical reinforcement, but that it is linked to a modification of the polymer chains dynamics.[1–4] Several NMR measurements have indeed shown the presence of slowed-down polymer in filled elastomers.[5–10] The presence of fillers thus modifies the polymer dynamics in the vicinity of the solid surfaces. This way, the fillers appear as a hard sphere with a soft shell dispersed in an even softer matrix.

The presence of the fillers also induces a non-linear mechanical behavior when the filled elastomers are solicitated at high strain amplitudes: the elastic modulus decreases substantially above a few percents of strain.[11] This is called the Payne effect and it is at the origin of energy dissipation. It is essential to better understand this effect for example to help reduce fuel consumption in vehicles. One important feature of the Payne effect is that its amplitude is strongly linked to the dispersion state of the fillers. Studying filled elastomers with the same physical chemistry but different dispersion states, we showed that the better the dispersion, the lower the Payne effect amplitude.[12] We thus see that the distance between particles is a crucial parameter and that it will be important to compare it to the range of polymer dynamics modification in order to understand the mechanical behavior of filled systems.

In this perspective, we combine in this paper results from various experimental measurements done on the same model filled elastomers: NMR measurements giving access to the amount of immobilized polymer,[13,14] SANS experiments giving information on the fillers dispersion and rheometry measurements enabling the determination of the Payne effect amplitude. Our objective here is to compare the range of the polymer dynamics modification to the distance between particles, to see if immobilized polymer is connecting the particles to each other and if it is correlated with the apparition of a significant Payne effect. We see here that it will be crucial to interpret the SANS

[a]*PPMD-SIMM, Soft Matter Science and Engineering, UMR 7615 CNRS/UPMC/ESPCI ParisTech, 10 rue Vauquelin, F-75231 Paris Cedex 5, France. E-mail: aurelie.papon@espci.org; Web: www.ppmd.espci.fr/?lang=en*
[b]*Laboratoire Charles Coulomb UMR 5221 CNRS-UM2, Département Colloïdes, Verres et Nanomatériaux, Université Montpellier II, 34095 Montpellier Cedex 05, France. E-mail: Julian.Oberdisse@univ-montp2.fr*
[c]*Institut für Physik – NMR, Martin-Luther-Universität Halle-Wittenberg, Betty-Heimann-Str. 7, D-06120 Halle, Germany*
[d]*Rhodia Opérations, 15 rue Pierre Pays, BP 52, F-69660 Collonges-au-Mont-d'Or, France*

data in a very careful way, in order to obtain the distribution of distances between particles, and not simply a mean value. That is why we propose here to interpret them through reverse Monte-Carlo simulations, which will give us access to a representative configuration of the particles in each sample.

Finally, from the reverse Monte-Carlo (RMC) simulations used to interpret SANS data, we get the distances between particles. Then, from the two sets of results obtained from NMR measurements on the same samples we determine the range of the polymer dynamics modification. Combining the two previous results, we estimate the number of connections by immobilized polymer between particles. We propose a rescaling of the Payne effect as a function of the number of immobilised bridges per particles. Our results show that the presence of immobilized "bridges" between particles is a key parameter to explain the Payne effect. The paper is organized as follows. We briefly recall the materials and methods we have used—all the samples having extensively described in previous publications. We then explain how, from RMC simulations, we extract the spatial arrangements of particles from small angle neutron scattering. Secondly we recall and discuss the results of two types of nuclear magnetic resonance (NMR) measurements that have been performed on these samples with two different time windows. Lastly we link the two previous sets of data with the Payne effect results, and propose to relate the number of immobilized polymer bridges per particles to the Payne effect amplitude. We then discuss the implication of this relation and conclude on the existence of a long range temperature dependent mechanical interaction between neighboring particles through the polymer matrix of about typically 7 nm.

II. Materials and methods

Samples

All the samples used here are the same as the ones used in our previous studies.[12,13,15,16] The model filled elastomers consist of grafted silica particles dispersed in a poly(ethylacrylate) matrix. Two kinds of grafter have been used: TPM (3-(trimethoxysilyl) propyl methacrylate), which can react with the monomer and thus create a covalent bond with the matrix, and C8TES (n-octyltriethoxysilane) with which there are only hydrogen bonds between the residual –OH groups on the silica surface and the polymer. The synthesis process has been described elsewhere.[15] The main characteristics of the samples studied are given in Table 1. Note in all the considered experiments, the samples can be considered as annealed, and we have checked that there is neither an effect of annealing at high temperature nor of swelling/deswelling by solvents.

SANS

Small angle neutron scattering was performed on beamlines D22 at Institut Laue-Langevin (ILL), KWS2 at IFF-Juelich and PAXY at Laboratoire Léon Brillouin (LLB). The measured intensities were calibrated to an absolute standard in order to get absolute units.[15] The incoherent background was estimated from the known high-q Porod law of silica particles. The contrast observed in our samples is only between polymer and silica, we do not see any contrast between glassy and network-like polymers for example.

III. Results

A. Filler arrangement: reverse Monte-Carlo simulations on SANS measurements

The dispersion of silica nanoparticles in a nanocomposite can be characterized by small angle neutron scattering. For monodisperse assemblies of spheres, the resulting intensity $I(q)$ can be factorized in form and structure factors, $P(q)$ and $S(q)$, respectively. For weak polydispersities, which is the case for our samples (about 10%), this equation is usually used, and can be justified *a posteriori* with the resulting nearest neighbor statistics (*e.g.* Table 1), which shows that only rarely particles close enough that small size variations would matter. $P(q)$ can be measured independently in dilute solution, and $S(q)$ contains information on the dispersion, because it is the Fourier transform of the pair correlation function of the particles (see Fig. 1). In this context, the goal of a reverse Monte-Carlo (RMC) analysis is to find a representative configuration of the nanoparticles by a random exploration of phase space, which is in agreement with the experimentally measured structure factor.[17–20]

In practice, a 3D simulation box of linear dimension L is filled with N_{tot} nanoparticles, such that the desired volume fraction of silica, ϕ_{Si}, is reached. The finite size of the box induces a low-q cut-off of the data (see Fig. 2 (b)), but bigger boxes (allowing a lower cut-off) need a higher calculation effort, and a compromise is sought. The position of the cut-off was evaluated using random dispersions, which highlight the finite-size contribution at low-q of the box (*e.g.* its form factor oscillations at low-q visible in Fig. 2b). The initial configuration can be of any type, as long as the excluded volume condition of the silica spheres is respected. Weak polydispersity of the particles can also be introduced at this stage. Then the system is allowed to rearrange in order to satisfy the structure as measured by $I(q)$. To this aim, the pair correlation function is calculated and Fourier transformed.[21] The resulting prediction for the structure factor $S_{sim}(q)$ is compared to the experimental one:

$$\chi^2 = \frac{1}{n}\sum_{i=1}^{n}\left(\frac{S(q_i) - S_{sim}(q_i)}{\Delta S}\right)^2 \quad (1)$$

In eqn (1) n denotes the number of intensity data points, and ΔS the possibly q-dependent error bar on the structure factor. In order to minimize χ, a series of Monte-Carlo steps is performed: a particle is chosen randomly, and moved by a fixed step-length in a random direction, respecting the excluded particle volume. For the step length, a compromise (0.5 nm) was used. The step is much smaller than the particle radius to allow a detailed exploration of parameter space, but large enough to make the algorithm converge in a reasonable calculation time. Then χ is reevaluated, and the step is accepted according to a Boltzmann criterion. If χ has decreased or increased marginally with respect to the "Boltzmann" parameter ε, the step is accepted: $exp\left(-\frac{\Delta\chi}{\varepsilon}\right)$ must be larger than a random number between 0 and 1. Otherwise, the step is refused. In the course of the simulation, agreement between the prediction and the observed structure, ε, which plays the role of a temperature in a simulated annealing procedure, is progressively decreased, until a minimum value which ensures some fluctuations of the structure around

Table 1 Sample characteristics: silica particle diameter, silica volume fraction, distance between neighboring particles (surface to surface) according to the reverse Monte-Carlo simulations (RMC), a random close packing arrangement (RCP) and the number or first neighbors according to the RMC simulations

Sample name	Si diam. (*nm*)	Si vol. fraction	h_{RMC} (nm)	h_{RCP} (nm)	Number of first neighbors
T30 TPM 30	27	0.20	3	12.6	2
T30 TPM 25	27	0.16	3	15.6	2
T30 TPM 18	27	0.11	2	21.1	1
T50 TPM 30	43	0.22	21	18.8	12
T50 TPM 25	43	0.15	34	27.3	14
T50 TPM 18	43	0.11	37	33.7	14
T100 TPM 30	83	0.29	30	25.1	11
T100 TPM 25	83	0.17	48	45.2	11
T100 TPM 18	83	0.12	57	60.4	11
T30 C8TES 30	26	0.17	6	15.4	5
T30 C8TES 25	26	0.15	6	16.4	4
T30 C8TES 18	26	0.10	6	22.0	3
T50 C8TES 44	42	0.29	4	12.2	5
T50 C8TES 30	42	0.18	4	21.7	3
T50 C8TES 25	42	0.15	7	25.1	3
T50 C8TES 18	42	0.10	7	33.9	2

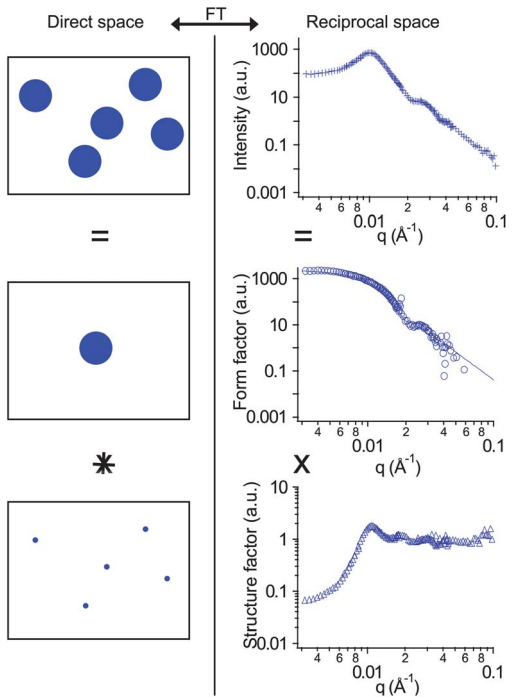

Fig. 1 SANS analysis. The intensity scattered by the silica particles is the product of the form factor of the particles (describing the shape and polydispersity of the fillers) by the structure factor, which describes the position of each filler. The transition from direct space to reciprocal space is obtained through a Fourier transform (FT). The form factor is experimentally measured on a diluted solution of silica particles, and in the following, we will only consider the structure factor in order to determine the fillers positions.

a representative structure. Once this plateau is reached, one obtains a series of three-dimensional representations of the nanoparticle arrangement in space, the scattering of which agrees with the experimental intensity. We checked that the simulations gave rise to equivalent final configurations *i.e.* lead essentially identical pair distribution functions (and thus scattering, peak heights and positions, *etc.*), independently of the choice of the initial value of ε.

The typical results of an RMC simulation are given in Fig. 2 for the sample T50 TPM 25. We used boxes with 8000 particles and we performed 1.6×10^7 steps in the simulation, so that a plateau in χ^2 is obtained. The number of particles is chosen to give access to representative configurations and reasonable simulation times. Increasing the number of particles further did not improve significantly enough the precision of the results compared to the required simulation time. We tested various initial configurations of the particles: random or crystalline, and we see in Fig. 2 (a), (b) and (c) that they gave rise to equivalent configurations at the end of the simulation. It thus shows the robustness of the method.

The main result we obtain from the RMC simulations is the pair correlation function of each sample, that is the probability to find a particle at a given distance r of another one. We note here that our model samples exhibit a certain order in their arrangement, which appears as oscillations in the pair correlation function. The first peak corresponds to the first neighbors, second peak to the second neighbors *etc.*

The simulations have been performed on all the samples and two parameters have been computed in order to compare them more easily: the number of first neighbors and the mean distance between neighboring particles. The mean distance between neighboring particles is obtained by direct calculation on the final configuration of the simulation box and the average number of first neighbors around a given particle, and is obtained by integration of the first peak (*fp*) of the pair correlation function $g(r)$:

$$z_n = \int_{fp} g(r) \frac{N_{tot}}{V_{tot}} 4\pi r^2 \mathrm{d}r \qquad (2)$$

The results are gathered in Table 1. The first and the second columns indicate respectively the diameter d of the silica particles and the silica volume fraction. The grafter is indicated in the name of the samples, TPM holding for a covalent grafting and C8TES for a non-covalent grafting. The value h_{RMC} indicates the

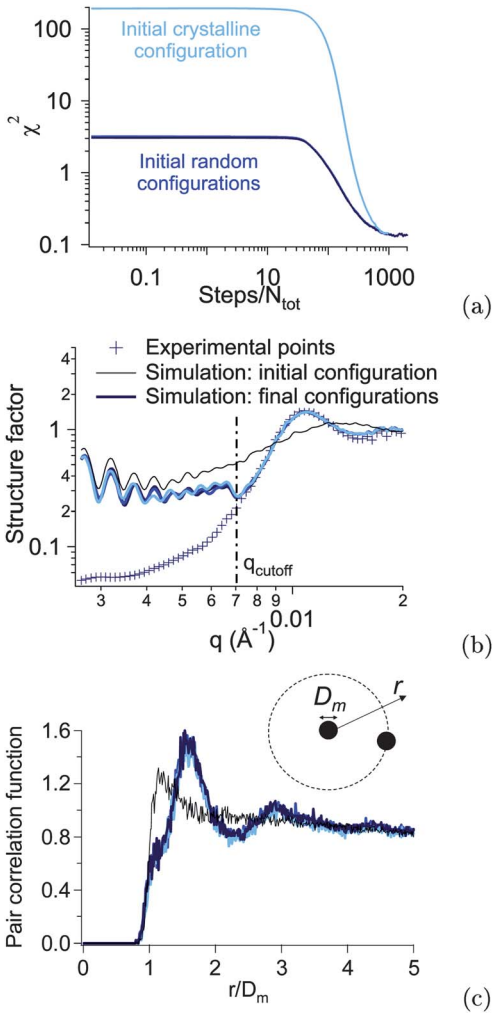

Fig. 2 RMC simulation results for different initial configurations, either crystaline (light blue) or random (dark blue). Number of particles = 8000, total number of steps = 1.6×10^7. (a) χ^2 as a function of the number of steps in the simulepsation normalized by the number of particles $N_{tot.}$ (b) Experimental (crosses) and simulated (lines) structure factors. The structure factor corresponding to the initial random configuration is shown with the thin line. (c) Pair correlation function in the initial (thin line) and final configurations (thick lines), as a function of r/D_m, the distance normalized by the mean diameter of the particles. We observe that the final configurations are equivalent, and thus independent of the initial configuration chosen.

average distance between the neighboring particles extracted from RMC. The value h_{RCP} is the distance between particle that would be observed in the case of a random close packing arrangement of particles of diameter $d + h_{RCP}$. The last column indicates the average number of first neighbor around a given particle, and is obtained by the integration of the pair correlation function. We see that the samples can be split in two main groups. Samples T50 TPM and T100 TPM have a high number of first neighbors at a rather large distance between neighboring particles, which is characteristic of a good dispersion state, whereas the other samples have only few neighbors in close vicinity, meaning that they are not so well dispersed. As an example, Fig. 3 (a) is a 3D representation of the first and second neighbors of a silica particle in the sample MIST TPM 30, as

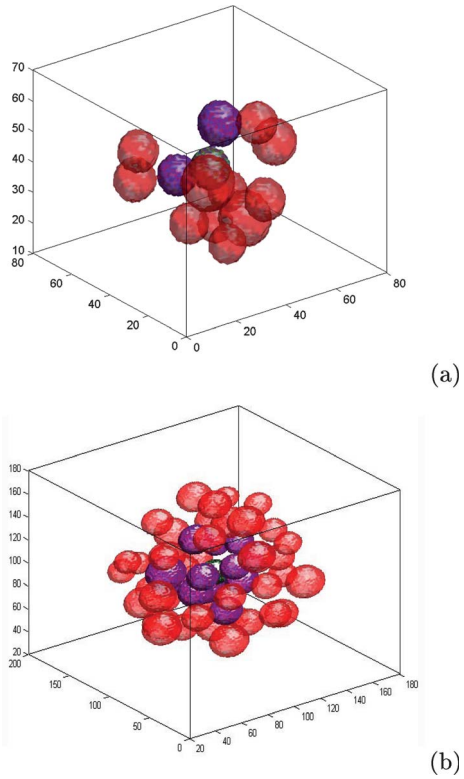

Fig. 3 3D representation of the silica particles arrangement in the samples MIST TPM 30 (a) and T50 TPM 30 (b) (at different scales). A particle is chosen—in green—and its first neighbors are represented in blue and the second ones in red.

obtained after the simulation. We see that the particles are almost in contact with each other. On the contrary, Fig. 3 (b) shows that the first neighbors of a silica particle in the sample T50 TPM 30 are much further away from each other.

Even if all the samples exhibit rather well dispersed particles (no aggregates), we see that it will be important to take into account the difference in their configurations in order to compute the number of possible of connections between particles by immobilized polymer.

As the polymer dynamics is modified in the vicinity of solid surfaces, it will also be important, for the interpretation of the NMR data, to know the polymer volume fraction situated at a given distance z from the nearest solid surfaces. A typical curve, obtained from the particles configuration after simulation, is given in Fig. 5 (a) and is compared with an isolated particle hypothesis. We will come back to this curve in the next section.

B. Range of the polymer dynamics slowing-down induced by the fillers

Recall on the ^{1}H NMR measurements. We have recently proposed two different sets of solid ^{1}H-NMR measurements done on the same model filled elastomers. In these measurements, we are interested in the free induction decay (FID) of the protons of the systems—sensitive to the mobility of the spins—over two different time windows. The rather long dead time of the NMR device, which prevents the recording of the beginning of the FID, is overcome by refocussing the FID with a magic

sandwich echo (MSE) pulse sequence. The sequence is described in more detail in ref. 13. At a temperature high enough above the glass transition temperature T_g, a pure elastomer exhibits a MSE-FID signal that is a slowly decaying nearly exponential signal with a characteristic time above 0.10 ms. Below T_g, that is in the glassy state, the MSE-FID signal is Gaussian with a characteristic time around 20 μs. For the filled elastomer at temperatures above T_g, we observe a signal that is nearly exponential at long timescales, but with a Gaussian initial decay, showing the presence of immobilized—most probably glassy—polymer in filled elastomer even above T_g (see Fig. 4). To interpret the MSE-FID signal of the filled elastomers, we used two types of description: one based on a T_g gradient in the vicinity of the solid surfaces,[14] as it has been observed in thin polymer films,[22] and one based on the presence of three polymer dynamics in the samples: one glassy, one elastomer and one intermediate,[13] similar to the interpretation proposed by Kaufman.[5] We will show in this section that even if that this two analysis may seem at first view incompatible, they are in fact complementary.

With the T_g gradient interpretation, we focussed on the presence of glassy polymer and thus on the α-relaxation of the polymer chains. The T_g gradient concept originates from the observation in thin polymer films of T_g shifts depending on the polymer thickness.[22] The interpretation and model developed in ref. 23 is based on the consideration that glasses are constituted, at small scales, of domains with very different dynamics. This description is consistent with the heterogeneous dynamics of glasses. In this approach, the glass transition consists in the appearance—at a given timescale and for a given temperature—of a percolation of the slow domains. This percolation is modified near a boundary, which leads to the following relationship for the glass transition temperature T_g at a distance z of a surface:

$$T_g(z) = T_g^{\infty}\left(1 + \frac{\delta}{z}\right) \quad (3)$$

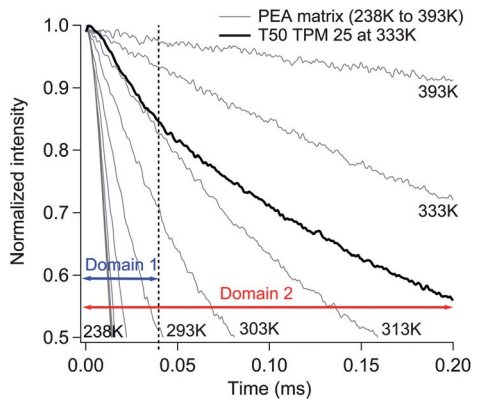

Fig. 4 MSE-FID signals of the pure PEA matrix between 238 K (T_g − 35 K) and 393 K (T_g + 120 K) and of one filled samples (T50 TPM 25) at 333 K. We see that the signal of the filled samples is nearly exponential at long timescales, and exhibits a more Gaussian shape at short timescales, showing the presence of immobilized polymer. The time domain 1 (0–40 μs) focuses on the α-relaxation, with a similar weight given to glassy and non-glassy polymer, whereas time domain 2 includes also polymer dynamics modification in the elastomer phase.

where T_g^{∞} is the glass transition temperature in the bulk and δ is a parameter of the gradient. In order to focus on this phenomenon, we have selected the time window 0–40 μs (time domain 1 in Fig. 4), where the relative weight of glassy and non-glassy polymer is of the same order of magnitude. Here, the T_g gradient starts at the surface of the grafters, that is at a distance e_0 of the silica surface. z is thus the distance from the grafters. The filled elastomer signal expected for this model is thus the integration around a silica particle of the signals of the protons of a pure matrix taking into account the change in $T_g(z)$, in addition to the immobilized protons of the grafters. With this model, we could fit the MSE-FID signals of filled elastomer on a wide range of temperature, with only two parameters: e_0 of the order of 1.5 nm for TPM grafter and 0.5 nm for C8TES grafter, in agreement with the grafting densities, and δ between 0.1 and 0.2 nm for all the samples. Moreover, we could still describe the NMR signals in the case of solvent addition, and the same parameters could be used to predict quantitatively the differential scanning calorimetry (DSC) response of the filled samples from the one of the matrix. The typical glassy thicknesses obtained (the criterion chosen is polymer below its T_g + 20 K) are between 2 and 6 nm between T_g + 120 K and T_g + 40 K). Hence, we have shown that part of the polymer in filled elastomers can be interpreted as glassy and that a T_g gradient model can quantitatively describe its behavior with temperature and solvent.

With this first interpretation, we are thus able to describe the α-relaxation near a surface. However, the polymer dynamics might be modified at a longer range in the elastomer phase, and in this case, we also have to take into account, for example, Rouse modes modifications. That is why, in ref. 13, we propose a second picture to describe the whole MSE-FID signals until 0.20 ms (time domain 2 in Fig. 4). Instead of a gradient of mobility, we propose here to use simply two or three kinds of mobilities. As a two-component model is not sufficient to give a satisfactory description of the signals near T_g, we use a model with three components: glassy (Gaussian signal), elastomer (exponential signal) and intermediate (stretched exponential signal). This analysis gives access to the volume fraction of each component as a function of temperature. With this appraoch, we call "immobilized" polymer the sum of the glassy and intermediate fractions.

Contribution of the RMC simulations in the computation of the range of slowed-down polymer dynamics. Regarding the first interpretation—T_g gradient model—the RMC simulations validate our approximation of the isolated particles hypothesis. Indeed, closer than 6 nm from a surface, the polymer volume fraction obtained in the particles configuration after RMC simulation is very close to the curve obtained in an isolated particle hypothesis. The glassy thicknesses computed with this model (2–6 nm) are thus confirmed.

For the second interpretation—the three components model—the RMC simulations enable the translation of the immobilized polymer volume fractions into thicknesses and thus the estimation of the range of the polymer dynamics modification. For that, we use the data—extracted from SANS measurements and reverse Monte-Carlo simulations—giving the polymer volume fraction at a distance z of a solid surface and deduce the thickness

corresponding to the glassy (ϕ_g) and immobilized (ϕ_{imm}) volume fractions (Fig. 5 (a)).

We then compare the results obtained from the two methods in Fig. 5 (b). First, we see that the T_g gradient indeed describes well the glassy polymer detected with the three components method. It validates the ability of this model to interpret the glassy dynamics in our model filled elastomers. Moreover, we see that another polymer dynamics modification occurs at longer scales and that it appears as the intermediate fraction in the second method. This longer range modification might be due to a modification of the Rouse modes of the chain and is most probably linked to change in the topological constraints felt by the polymer in presence of the fillers. In particular, for the samples with the covalent grafting agent (TPM), we have shown in ref. 13 that the effective density of topological constraints is higher than in the pure elastomer matrix. It is thus not surprising that the Rouse modes of the polymer chains are modified.

C. Link with the Payne effect

Let us first recall what the Payne effect is. Under sinusoidal strain oscillation, filled rubber samples exhibit—in a stationary situation—a nearly sinusoidal stress response and allow to measure an apparent viscoelastic modulus. However, in this regime, the amplitude of the elastic modulus—and also to a smaller extent of the loss modulus—depends on the amplitude, even for an amplitude as small as 10^{-4}. For the elastic modulus, this corresponds to a decrease of the elastic modulus that commonly called the Payne effect. This Payne effect is one of the major ingredients for the fuel consumption of cars. This phenomenon is related to the fact that some "links" between the fillers strain-soften under cyclic mechanical solicitation. Indeed it is commonly observed that under large enough strain amplitude, the apparent elastic modulus tends toward the one that would exhibit the matrix reinforced by solid particles but in the absence of any modification of the rigidity of the polymer phase by these particles.[11] Here we aim to understand how the Payne effect is related to the polymer dynamics modification observed by NMR. For that we will consider that particles connected by immobilized polymers form a network, that is able to be strain-soften by a cyclic strain.

Combining the results obtained in the two previous sections, we can compute the average number of either glassy or immobilized connections between particles, by integration of the pair correlation function up to a distance corresponding to the glassy or immobilized thickness. It gives thus the number of particles connected to a given one through glassy or immobilized polymer at a given temperature. We want now to see if there is a correlation between the quantity of connections between particles and the mechanical behavior of the samples, in particular with the amplitude of the Payne effect. We thus measured the amplitude of the Payne effect for all the samples. We will consider for the sake of simplicity the elastic modulus drop at a given strain amplitude (here 15%) at different temperatures. However in the following arguments, other values of strain amplitude could have been chosen without any loss of generality.

If we consider that the relevant bridges between particles are the one created by glassy polymer (e or e_g), we observe only very few connections between particles. On average, we find less than one connection per particle, which is thus not sufficient to explain a sensible change in the mechanical behavior of the samples. It is therefore more relevant to consider the polymer in the immobilized state (that is glassy + intermediate mobility $- e_{imm}$) and we present in Fig. 6 the amplitude of the Payne effect

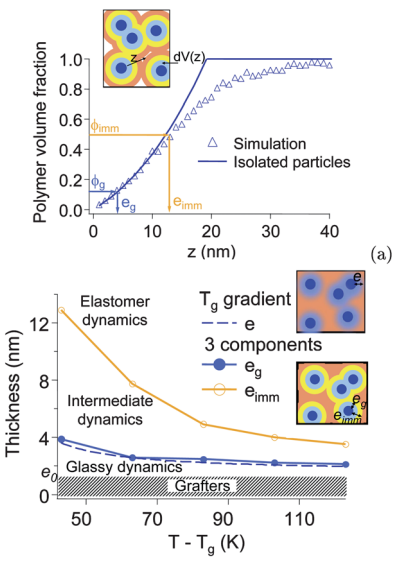

Fig. 5 Determination of the glassy and immobilized thicknesses. (a) Evolution of the polymer fraction corresponding to a certain thickness around each particle. Comparison of the isolated particles hypothesis (plain line) with the calculation obtained in the simulation box (triangles). Knowing the glassy and immobilized polymer volume fractions from the NMR measurements, we can now deduce the corresponding thicknesses e_g and e_{imm} respectively. (b) Glassy and immobilized thicknesses as a function of the temperature for the three-component analysis, compared with the thickness of polymer below its T_g + 20 K obtained with the T_g gradient model. We see that the T_g gradient model indeed describes well the glassy dynamics in filled elastomers and that the polymer dynamics is also modified on longer lengthscales and is seen as polymer with "intermediate" dynamics in NMR.

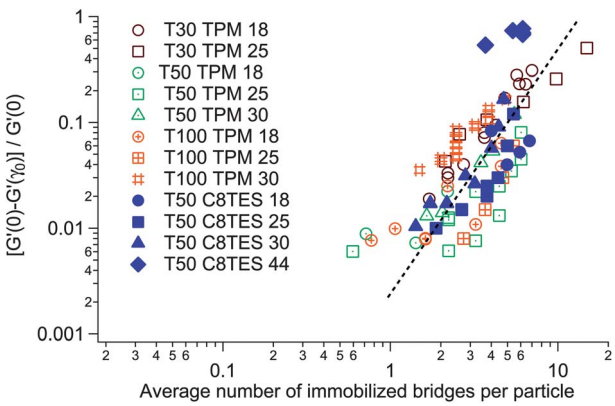

Fig. 6 Amplitude of the Payne effect as a function of the average number of immobilized bridges in various samples and several temperatures between 6 °C to 70 °C. The line is a guide for the eyes.

plotted as a function of the average number of immobilized bridges per particle for various samples and temperatures (taking into account the change in frequency and thus in T_g between mechanical and NMR measurements). We see here that the amplitude of the Payne effect indeed increases with the number of immobilized connections between particles for all the samples and that all the experimental points are rather well grouped together, independently of the size, volume fraction and exact dispersion state of the fillers. It is also important to note here that this observation is true for different types of interactions between the polymer and the filler: covalent links with the TPM grafter or H bonds for the C8TES grafter. Therefore, the amount of particles connected to each other by immobilized polymer seems to be a key parameter in the interpretation of the Payne effect of the samples.

IV. Discussion and conclusion

In this paper, we have put together results from various experimental technics in order to relate the mechanical behavior of filled elastomers to the dispersion state of the fillers and to the polymer dynamics in those systems. First, SANS experiments, interpreted through reverse Monte-Carlo simulations gave access to representative configurations of the fillers in our samples. Then, NMR measurements, interpreted with two different methods, put into light two kinds of polymer dynamics modification: at short lengthscales (polymer in the glassy state) but also at longer range (Rouse modes modification). We could estimate the range of the two types of dynamics modification. Putting together those two pieces of information, we could compute the quantity of particles connected to each other by glassy or immobilized polymer and relate it to the amplitude of the Payne effect at the same temperature. We observed that all the samples (with different filler–polymer interactions, various fillers sizes, contents and dispersion states) behaved in a similar way: the amplitude of the Payne effect increases with the quantity of immobilized connections bewteen particles. It shows thus that the mechanical behavior of the samples is sensitive to polymer dynamics modification at longer range than only glassy. Indeed, the presence of glassy polymer induces a slowing down of the polymer chains at longer range: if part of a polymer chain is in a glassy state, the rest of the chain might still feel this embedding, at least until the next cross-link or entanglement, which are estimated to have characteristic spacings of 7 nm and 10 nm respectively in our samples (see Fig. 7). And this longer range mobility restriction might indeed affect the mechanical behavior of the samples.

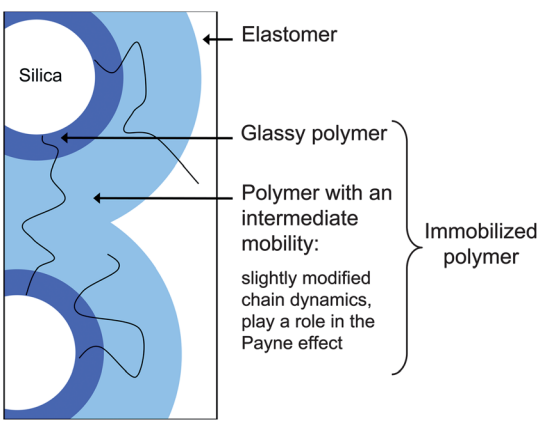

Fig. 7 Schematic representation of glassy and immobilized polymer.

In conclusion, this study permitted us to get a more global view of filled elastomers' behavior and to link their geometry and dynamics to their mechanical behavior. It showed the need to consider both the range of the polymer dynamics modification in the vicinity of the fillers and the distances between fillers in order to interpret the mechanical behavior of the systems.

Acknowledgements

We want to thank Didier Long, Anne-Caroline Genix and Christian Frétigny for many fruitful discussions. We gratefully acknowledge the financial support of the ANR grants TaylRub and DynaFil.

References

1 M. Wang, *Rubber Chem. Technol.*, 1998, **71**, 520.
2 L. Chazeau, J. Brown, L. Yanyo and S. Sternstein, *Polym. Compos.*, 2000, **21**, 202.
3 G. Heinrich and M. Kluppel, *Adv. Polym. Sci.*, 2002, **160**, 1.
4 M. Kluppel, *Adv. Polym. Sci.*, 2003, **164**, 1–86.
5 S. Kaufman, W. Slichter and D. Davis, *J. Polym. Sci., Part A-2*, 1971, **9**, 829.
6 J. Kenny, V. McBrierty, Z. Rigbi and D. Douglass, *Macromolecules*, 1991, **24**, 436.
7 Y. Ou, Z. Yu, A. Vidal and J. Donnet, *J. Appl. Polym. Sci.*, 1996, **59**, 1321.
8 V. Litvinov and P. Steeman, *Macromolecules*, 1999, **32**, 8476.
9 J. ten Brinke, V. Litvinov, J. Wijnhoven and J. Noordermeer, *Macromolecules*, 2002, **35**, 10026.
10 G. Leu, Y. Liu, D. Werstler and D. Cory, *Macromolecules*, 2004, **37**, 6883.
11 A. Payne, *Reinforcement of elastomers*, Interscience, New-York, 1965, ed. G Kraus.
12 H. Montes, T. Chaussee, A. Papon, F. Lequeux and L. Guy, *Eur. Phys. J. E*, 2010, **31**, 263.
13 A. Papon, K. Saalwächter, K. Schäler, L. Guy, F. Lequeux and H. Montes, *Macromolecules*, 2011, **44**, 913.
14 A. Papon, H. Montes, M. Hanafi, L. Guy, K. Saalwächter and F. Lequeux, *Phys. Rev. Lett.*, 2012, **108**, 065702.
15 J. Berriot, H. Montes, F. Martin, M. Mauger, W. Pyckhout-Hintzen, G. Meier and H. Frielinghaus, *Polymer*, 2003, **44**, 4909.
16 J. Berriot, F. Lequeux, L. Monnerie, H. Montes, D. Long and P. Sotta, *J. Non-Cryst. Solids*, 2002, **307–310**, 719.
17 R. L. McGreevy, *J. Phys.: Condens. Matter*, 2001, **13**, R877.
18 K. Hagita, T. Arai, H. Kishimoto, N. Umesaki, Y. Shinohara and Y. Amemiya, *J. Phys.: Condens. Matter*, 2007, **19**, 330017.
19 J. Oberdisse, P. Hine and W. Pyckhout-Hintzen, *Soft Matter*, 2007, **3**, 476.
20 O. Gereben, L. Pusztai and R. L. McGreevy, *J. Phys.: Condens. Matter*, 2010, **22**, 404216.
21 J. Hansen and I. R. McDonald, *Theory of simple liquids*, Academic Press, 2006.
22 D. Fryer, P. Nealey and J. de Pablo, *Macromolecules*, 2000, **33**, 6439.
23 D. Long and F. Lequeux, *Eur. Phys. J. E: Soft Matter Biol. Phys.*, 2001, **4**, 371.